Peptide Science

WILEY

PeptideScience

ARTICLE

Hierarchical Assembly of a Tetrameric Coiled-Coil Into Cuboid Structures

Ryan W. Curtis | Manish Nepal | Monessha Nambiar | Michael D. Jorgensen | Jean Chmielewski

560 Oval Drive, Department of Chemistry, Purdue University, West Lafayette, Indiana, USA

Correspondence: Jean Chmielewski (chml@purdue.edu)

Received: 11 September 2024 | **Revised:** 13 December 2024 | **Accepted:** 15 December 2024

Funding: This work was supported by National Science Foundation.

ABSTRACT

A tetrameric coiled-coil peptide, **TetNL**, is used herein as a building block for hierarchical assembly into higher order structures. Assembly within phosphate buffer (pH 7.4) led to the rapid formation of micron-sized fibers and cuboid structures, a process that could be shifted toward cuboid formation with agitation during the assembly process. Investigation of the packing of the cuboid assemblies by TEM demonstrated a regular banding pattern (4.6 nm) within the structures that was perpendicular to the length of the cuboids, a value that supports an end-to end organization of the tetrameric coiled coils along the blocks. SWAXS analysis supports that the internal packing of the tetrameric coiled coil building blocks is a close-packed hexagonal structure. These data represent an interesting comparison with a trimeric coiled coil peptide, **TriNL**, that forms hollow nanotubes with the same internal hexagonal packing. Modified **TriNL** has been used to generate numerous unique morphologies, and the data presented herein provide a distinct tetrameric building block that can also be exploited in this manner.

1 | Introduction

Precise engineering of biomaterials requires a comprehensive understanding of the relationship between molecular structure and self-assembling properties [1]. Peptides, facilitated by varied functionality present in natural amino acids, have been designed to self-assemble into a wide variety of functional materials [2, 3]. A useful characteristic of peptides is that they can be designed to adopt stable secondary structures that subsequently undergo hierarchical self-assembly into higher ordered structures [4–6]. In particular, coiled-coil peptides are an intriguing structure due to the breadth of knowledge about the properties affecting their oligomerization state [7]. The identity of the amino acids along the hydrophobic face of the alpha helices and the interhelical residues dictate the orientation and oligomerization of the coiled-coil unit. Altering the oligomerization state of self-assembling coiled-coil peptides has previously been shown to affect their assembly properties [8–14], although there is significantly more sequence and structural space to explore.

In this regard, a coiled-coil peptide of note is that from the leucine zipper region of the GCN4 transcription factor. This peptide has been shown to adopt dimeric through tetrameric oligomeric states based on the identity of the amino acids in the hydrophobic core and solvent-exposed residues of the coils [15, 16]. A GCN4 coiled coil mutant with eight Ala residues has also demonstrated higher oligomerization to a seven-helix coil [17]. Specifically, a trimer is formed when the *a* and *d* positions are populated by isoleucine residues, whereas when these residues are leucine and isoleucine, respectively, a tetrameric coiled-coil predominates (Figure 1). This programmability creates a useful toolbox of different coiled-coil oligomers that can be harnessed for hierarchical assembly into functional materials.

The trimeric coiled-coil peptide, **TriNL** (Figure 1), for instance, has served as a versatile building block for inclusion of higher order assembly signals within the sequence [18–24]. On its own, **TriNL** has been observed to assemble into hollow

	abcdefg	abcdefg	abcdefg	abcdefg	abc
TetNL	Ac-**M**KQI**E**DK	LEEI**L**SK	LYHI**E**NE	LARI**K**KL	LGE-NH_2
TriNL	Ac-**M**KQI**E**DK	IEEI**L**SK	IYHI**E**NE	IARI**K**KL	IGE-NH_2

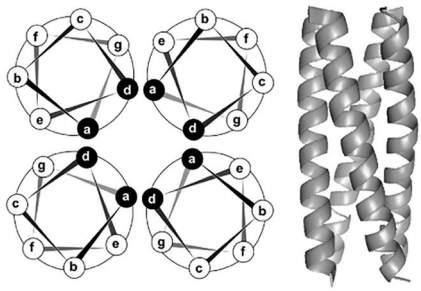

FIGURE 1 | (Top) Sequences of **TetNL** (tetramer) and **TriNL** (trimer) coiled-coil peptides indicating the heptad repeats (*a*-*g*). Residues in bold (*a* and *d*) comprise the hydrophobic core of the oligomer. (Bottom) A helical wheel diagram of a tetramer and coiled coil structure of **TetNL** [14].

nanotubes capable of encapsulating cargo, including proteins, dextrans, and fluorophores [14]. Incorporating ligands for metal ions at the termini of **TriNL** rapidly produced micron-sized hexagonal crystals and disks in a metal-dependent fashion, along with the ability to include His-tagged cargo within the crystals [25, 26]. Placing hydrophobic bipyridyl groups at the center of the **TriNL** sequence promoted assembly into banded nano- and microstructures, in a reversible, pH-dependent, fashion [23]. Addition of both of these terminal and central modifications within **TriNL** produced a complex three-dimensional matrix upon addition of metal ions, which encapsulated cells and supported their growth [24]. With this rich set of morphologies and function obtained starting from the **TriNL** building block, we hypothesized that the tetrameric variant, **TetNL** (Figure 1), may exhibit unique self-assembling properties due to inter-coiled-coil interactions from the additional α-helix. Herein, we explore the hierarchical assembly of the **TetNL** peptide and evaluate morphological changes brought about by the increase in the coiled-coil oligomerization state.

2 | Materials and Methods

2.1 | Materials

Fmoc (fluorenylmethyloxycarbonyl) -protected amino acids Fmoc-Gly-OH, Fmoc-Met-OH, Fmoc-Ser(tBu)-OH, Fmoc-Asn(Trt)-OH, Fmoc-Glu(OtBu)-OH, Fmoc-Gln(Trt)-OH, Fmoc-Tyr(tBu)-OH, Fmoc-Asp(OtBu), Fmoc-Ala-OH, Fmoc-Lys(Boc)-OH, Fmoc-Leu-OH, Fmoc-Ile-OH, Fmoc-His(Trt)-OH, and Fmoc-Arg(Pbf)-OH were purchased from ChemPep Inc. (Wellington, Florida, USA). HBTU (hexafluorophosphate benzotriazole tetramethyl uronium) was purchased from Chemimpex (Wood Dale, Illinois, USA). H-Rink Amide NovaPEG resin (LL) was purchased from Millipore Sigma. N,N-dimethylformamide (DMF), dichloromethane (DCM), methanol (MeOH), diisopropylethylamine (DIEA), trifluoroacetic acid (TFA), triisopropylsilane (TIPS), acetic anhydride, and diethyl ether were purchased from Sigma-Aldrich (St. Louis, Missouri, USA). Reagents purchased from commercial sources were used without further purification.

2.2 | Synthesis of TetNL

The synthesis of the **TetNL** peptide was performed using standard Fmoc (fluorenylmethyloxycarbonyl) based solid-phase synthesis methods on the NovaPEG Rink Amide resin (300 mg, 60 μmol). The resin was treated with the desired Fmoc-protected amino acid (4 eq., 240 μmol), HBTU (4 eq., 240 μmol), and DIEA (8 eq., 480 μmol) in DMF for 45 min at room temperature. The resin was washed with DMF, DCM, MeOH, DCM, and DMF (2 X 8 mL). The Fmoc protecting group was removed with a 20% piperidine solution in DMF (8 mL) for 20 min. After piperidine treatment, the resin was washed with DMF, DCM, MeOH, DCM, DMF (2 X 8 mL). This process was repeated until all the amino acids in the peptide were added to the resin. After the last Fmoc was deprotected, the N-terminus of the resin-bound peptide was acetylated with a solution of 5% acetic anhydride and 8.5% DIEA in DMF (8 mL) over 30 min. The resin was washed as described above.

The peptide was cleaved from the solid support with a solution of 95% TFA, 2.5% TIPS, and 2.5% H_2O (15 mL). The filtrate was collected, and the resin was washed with TFA (2 X 15 mL) and DCM (2 X 15 mL). The filtrates were combined, and the solvents were removed under reduced pressure. The peptide was precipitated using cold diethyl ether and collected via centrifugation. The peptide was purified to homogeneity by reverse phase (RP) HPLC on a Luna C18 semi-prep column (250 x 21.20 mm, 100 Å pore size, 10 μm, Phenomenex) using a using a solvent gradient of 20%–70% acetonitrile in H_2O (with 0.1% TFA) for 60 min. HPLC retention time: 34.5 min. The peptide was found to be greater than 95% pure by UPLC, and MALDI-ToF mass spectrometry confirmed the desired mass: calculated—3766.5, observed—3764.7. The concentrations of peptide solutions were determined using an Agilent Cary 6000i UV–Vis–NIR spectrophotometer based on the absorbance of tyrosine at 280 nm.

2.3 | Peptide Assembly

A 1 mM solution of **TetNL** was prepared in 200 mM of the indicated buffer (total volume: 50 μL) and incubated at room temperature for 1 or 24 h. In the case where the assembly process was agitated, the tube was placed in a rotary spinner for 1 h. In all cases, a precipitate formed immediately. At the indicated time, the precipitate that formed was collected by centrifugation (10,000 g, 3 min). The supernatant was removed, and the precipitate was re-suspended in water. The washing process was repeated three times to remove excess buffer. The assemblies were stored in water until analysis.

2.4 | Scanning Electron Microscopy (SEM)

TetNL samples were prepared for SEM by adding 5 μL of sample suspended in water onto a glass cover slip adhered to the stub with double sided copper tape. The samples were air-dried

and sputter coated with platinum for 60 s. Samples were imaged using a Teneo Volumescope SEM (FEI Company, Hillsboro, OR, USA) with an Everheart Thornley detector. Samples were acquired using an accelerating voltage of 5 kV with a working distance of 10 mm.

2.5 | Transmission Electron Microscopy (TEM)

TetNL samples were prepared for TEM by adding 5 μL of sample suspended in water to a 400-mesh copper grid coated in formvar with a carbon film that was previously glow discharged. The samples were left to stand for 10 min and the water was then wicked away. The grid was rinsed through stain droplets of 2% uranyl acetate and blotted dry. Samples were imaged using a Tecnai T20 TEM (FEI Company, Hillsboro, OR, USA) operated at 100 kV, with a spot size of 3200 μm condenser aperture and a 70 μm objective aperture. Images were captured using an SIA L3C 4-megapixel CCD camera.

2.6 | Small and Wide Angle X-Ray Scattering (SWAXS)

TetNL samples were prepared for x-ray scattering by dropping a 1 μL aliquot of the sample in water on scotch tape and allowing the sample to air dry. The measurements were performed using an Anton-Paar SAXSpoint 2.0 system with a Cu x-ray source. Diffraction patterns were acquired with an average of 3x15 minute scans using a 2D EIGER R series hybrid photon counting detector and a high-resolutions WAXS module. Measurements were obtained at a sample to detector distance of 113 nm.

3 | Results & Discussion

3.1 | Peptide Self-Assembly and SEM Analysis

The assembly properties of the tetrameric TetNL peptide were investigated. The peptide (1 mM) in phosphate buffer (pH 7.5) produced a visible precipitate within minutes. After 1 h at room temperature, the precipitate was collected and visualized by scanning electron microscopy (SEM). Interestingly, two major morphologies were observed. Thin micron-sized fibers had assembled, in addition to distinctive rectangular cuboid structures that ranged in length from 2 to over 30 μm (Figure 2a,b), with an average length of 15.8 ± 13.8 μm ($N = 30$). These structures represent a notable change in morphology from the hollow tubes formed by the trimeric coiled-coil **TriNL** [14]. Since there were two distinct populations of materials, we probed if a longer incubation time of the peptide in buffer would influence the distribution of the assemblies. **TetNL** was incubated, therefore, in phosphate buffer for 24 h. The peptide again generated cuboid structures with a similar size as compared to the 1 h experiments, with an average length of 18.1 ± 12.7 μm ($N = 30$). With the longer incubation time, however, there was notably more fiber-like structures coating the cuboids. (Figure 2c,d).

Due to the observation that two distinct morphologies were formed, we looked to explore methods to create a monodisperse assembly. In some cases, the characteristics of self-assembling peptides have been altered by constant agitation during the assembly process [27–29]. With this in mind, we subjected the **TetNL** peptide in buffer to agitation by rotating the mixture during the 1 h incubation period. The resulting structures were found to be much more monodisperse and the majority of the assemblies were smaller blocks (Figure 3), with an average size

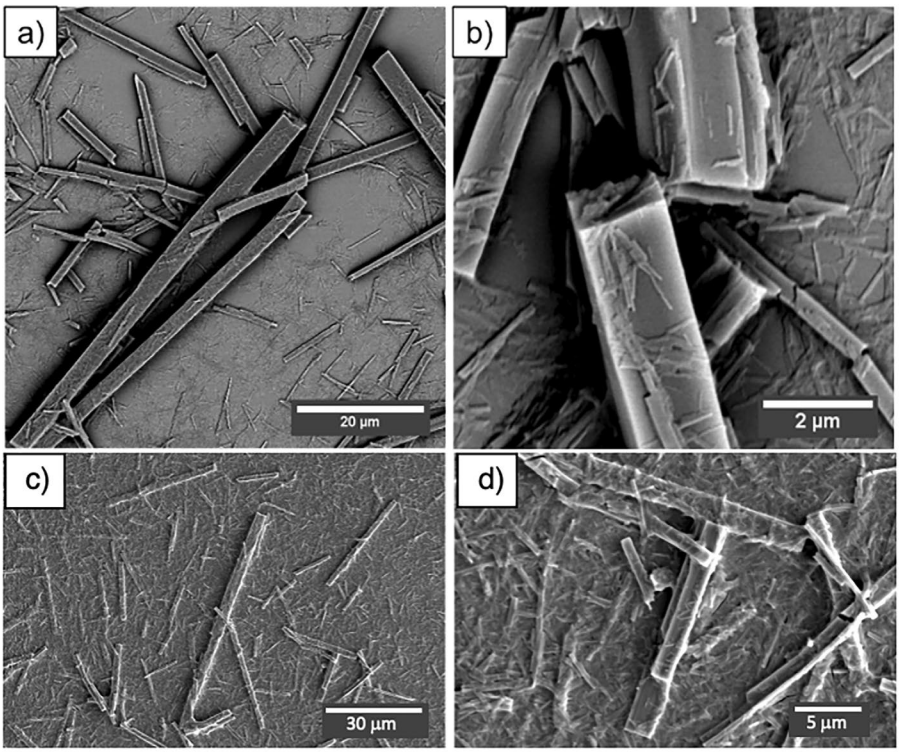

FIGURE 2 | SEM images of structures formed from **TetNL** (1 mM) assembled in phosphate buffer (200 mM, pH 7.5) for (a-b) 1 h and (c-d) 24 h.

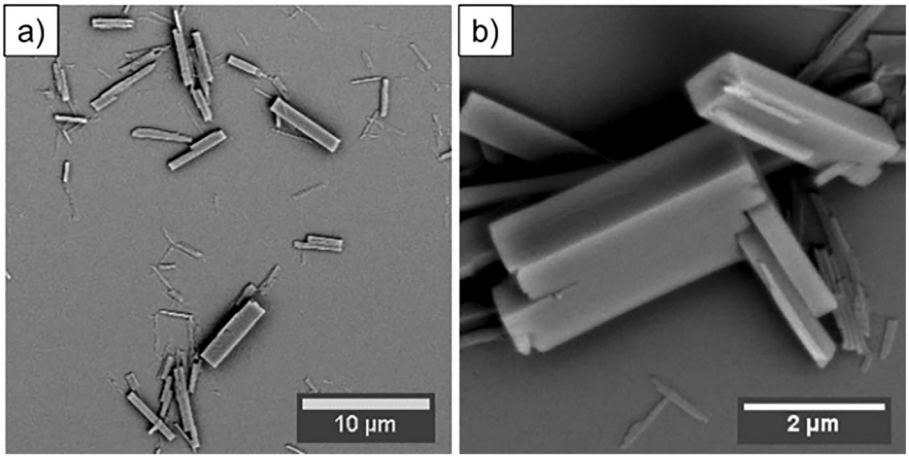

FIGURE 3 | SEM images of blocks formed by **TetNL** (1 mM) in phosphate buffer (200 mM, pH 7.5) for 1 h with constant mixing.

of 1.9 ± 0.7 μm ($N = 30$). This mechanical agitation may facilitate the assembly process by bringing the peptide in solution in more constant contact with the nucleating structure. A more rapid nucleation process has been shown to lead to more monodisperse molecular self-assembly [30].

It has previously been observed that coiled-coil peptides exhibit different self-assembling properties depending on the pH of the solution in which they assemble [31–35]. Therefore, we incubated **TetNL** (1 mM) in different buffers to probe this pH dependence. At pH values below the pKa of carboxylic acids (citrate buffer pH 3.8) or above the pKa of amines (CAPS buffer pH 11.8), no assembly was detected after 24 h. These data suggest that electrostatic interactions between charged side chains of coiled-coils play a role in the observed assembly process.

3.2 | Structural Analysis by TEM and SWAXS

These smaller, monodisperse blocks were studied further to investigate how the coiled-coil building blocks are arranged within the cuboids. The assemblies were first observed with transmission electron microscopy (TEM). This analysis revealed a distinct banding pattern perpendicular to the length of the rectangular blocks (Figure 4a). Fourier transform of the TEM images (Figure 4b) showed that the banding pattern repeated every 4.6 nm, which is about the length of the GCN4 tetramer [15]. This 4.6 nm length is shorter than what one would expect for a helical peptide of this size, presumably due to the supercoiling of the coiled coil structures. These data suggest that like **TriNL**, the **TetNL** coiled-coils are arranged along the length of the self-assembled structures (Figure 4c).

The cuboids were also examined with small and wide-angle X-ray scattering (SWAXS) (Figure 5a). The diffraction peak at $q = 1.40\,\text{nm}^{-1}$ corresponds to a d-spacing of 4.5 nm and is close to the length of the tetrameric GCN4 coiled-coil determined by X-ray crystallography [15], and TEM as described above. The distinct signals at q values of 3.11, 5.54, 6.31 nm^{-1} correspond to d-spacings of 2.02 nm, 1.13 nm and 1.00 nm, respectively. These data correspond to the (100), (110), and (200) planes in a hexagonal lattice with a lattice parameter of

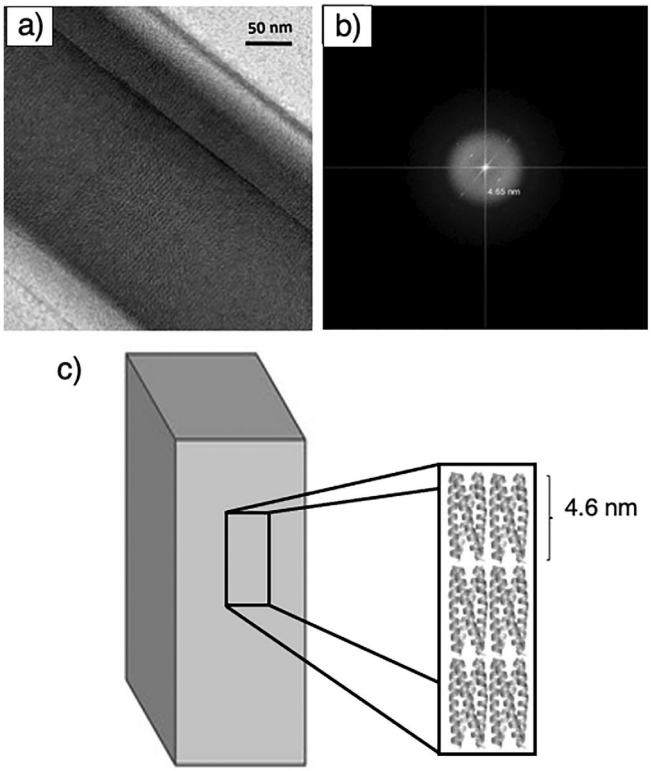

FIGURE 4 | (a) TEM image of a block formed by **TetNL** (1 mM) in phosphate buffer (200 mM, pH 7.5) for 1 h with constant mixing and (b) Fast fourier transform of the TEM image. (c) Representation of a self-assembled cuboid denoting the putative end-to-end assembly of **TetNL**.

2.33 nm (Figure 5b). Due to a low signal-to-noise ratio, we were not able to fit the low q values to a particular structure. Due to the size of a coiled-coil tetramer, the SWAXS data suggests that the coiled-coil units are arranged in a hexagonal close-packed arrangement. x-ray scattering combined with TEM analysis suggests that the tetramers are aligned end-to-end along the block and laterally in a hexagonal arrangement (Figure 5b). This is similar to the packing arrangement observed within the hollow nanotubes of **TriNL** (lattice parameter of 2.09) [14], although due to the extra alpha helix per coiled coil present in **TetNL**, the tetrameric oligomer packs into a larger hexagonal

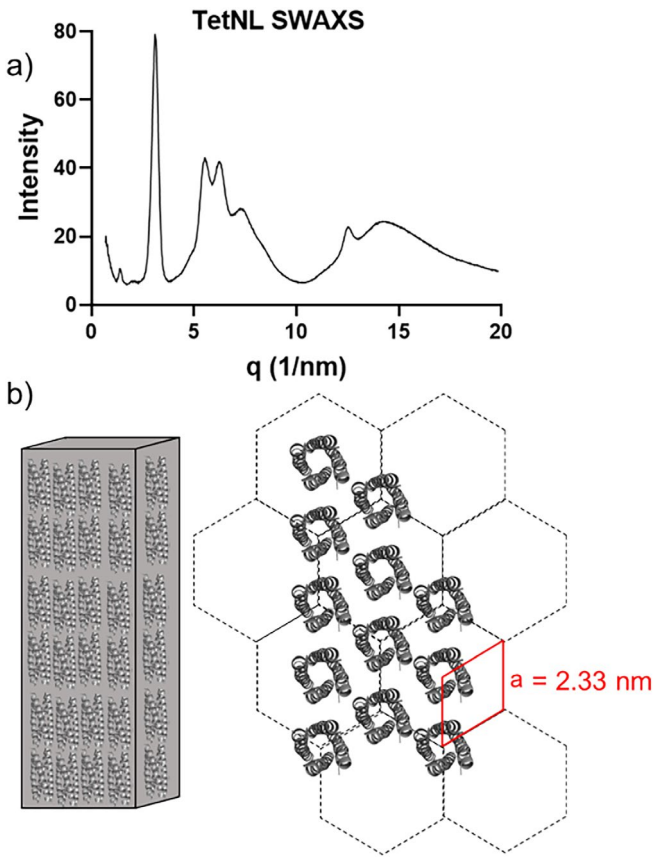

FIGURE 5 | (a) Small and wide-angle scattering (SWAXS) plot of the cuboids formed by **TetNL** (1 mM) in phosphate buffer (200 mM, pH 7.5) for 1 h with constant mixing and (b) the representation of proposed packing of the coiled-coil tetramers in the cuboid structures with a close-packed hexagonal organization.

lattice. Interestingly, the change from a trimeric to tetrameric building block with **TriNL** and **TetNL** leads to a dramatic change in morphology, from hollow nanotubes to rectangular cuboids, yet their internal packing remains fairly consistent. The q value of 12.51 nm^{-1} from the SWAX data corresponds to a d-spacing of 0.50 nm which could be attributed to hydrogen bonding or electrostatic interactions between the coiled-coils.

4 | Conclusion

In conclusion, a change in the coiled-coil oligomeric state, from trimer to tetramer, led to a considerable difference in the morphology of self-assembled materials. However, despite the change in morphology from nanotubes to rectangular cuboids with **TriNL** and **TetNL**, respectively, the internal organization of the coiled-coils maintained a hexagonal close-packed arrangement, implying that there may be a thermodynamic preference for hexagonal arrangement of GCN4-based coiled-coil assemblies. We also demonstrated that agitation during assembly leads to the formation of smaller, more monodisperse structures, presumably due to increasing the rate of coiled-coil assembly. Additionally, changes in the pH of buffers highlighted the importance of the charge of side chains on radially directed coiled-coil peptide assembly. In all, these studies further our understanding of the self-assembling properties of coiled-coil building blocks and will help direct the development of novel biomaterials in the future.

Acknowledgements

This work was funded by the National Science Foundation (CHE-2108722).

Conflicts of Interest

The authors declare no conflicts to interest.

References

1. S. Zhang, "Fabrication of Novel Biomaterials Through Molecular Self-Assembly," *Nature Biotechnology* 21, no. 10 (2003): 1171–1178, https://doi.org/10.1038/nbt874.

2. C. J. C. Edwards-Gayle and I. W. Hamley, "Self-Assembly of Bioactive Peptides, Peptide Conjugates, and Peptide Mimetic Materials," *Organic & Biomolecular Chemistry* 15, no. 28 (2017): 5867–5876, https://doi.org/10.1039/C7OB01092C.

3. P. Katyal, M. Meleties, and J. K. Montclare, "Self-Assembled Protein- and Peptide-Based Nanomaterials," *ACS Biomaterials Science & Engineering* 5, no. 9 (2019): 4132–4147, https://doi.org/10.1021/acsbiomaterials.9b00408.

4. D. N. Woolfson, "Building Fibrous Biomaterials From α-Helical and Collagen-Like Coiled-Coil Peptides," *Biopolymers* 94, no. 1 (2010): 118–127, https://doi.org/10.1002/bip.21345.

5. R. W. Curtis and J. Chmielewski, "A Comparison of the Collagen Triple Helix and Coiled-Coil Peptide Building Blocks on Metal Ion-Mediated Supramolecular Assembly," *Peptide Science* 113 (2021): 113 (2), https://doi.org/10.1002/pep2.24190.

6. M. D. Jorgensen and J. Chmielewski, "Recent Advances in Coiled-Coil Peptide Materials and Their Biomedical Applications," *Chemical Communications* 58, no. 83 (2022): 11625–11636, https://doi.org/10.1039/D2CC04434J.

7. J. M. Fletcher, A. L. Boyle, M. Bruning, et al., "A Basis Set of de Novo Coiled-Coil Peptide Oligomers for Rational Protein Design and Synthetic Biology," *ACS Synthetic Biology* 1, no. 6 (2012): 240–250, https://doi.org/10.1021/sb300028q.

8. D. V. Zaytsev, F. Xie, M. Mukherjee, et al., "Nanometer to Millimeter Scale Peptide-Porphyrin Materials," *Biomacromolecules* 11, no. 10 (2010): 2602–2609, https://doi.org/10.1021/bm100540t.

9. N. C. Burgess, T. H. Sharp, F. Thomas, et al., "Modular Design of Self-Assembling Peptide-Based Nanotubes," *Journal of the American Chemical Society* 137, no. 33 (2015): 10554–10562, https://doi.org/10.1021/jacs.5b03973.

10. N. A. Tavenor, M. J. Murnin, and W. S. Horne, "Supramolecular Metal-Coordination Polymers, Nets, and Frameworks From Synthetic Coiled-Coil Peptides," *Journal of the American Chemical Society* 139, no. 6 (2017): 2212–2215, https://doi.org/10.1021/jacs.7b00651.

11. J. Ang, D. Ma, B. T. Jung, S. Keten, and T. Xu, "Sub-20 Nm Stable Micelles Based on a Mixture of Coiled-Coils: A Platform for Controlled Ligand Presentation," *Biomacromolecules* 18, no. 11 (2017): 3572–3580, https://doi.org/10.1021/acs.biomac.7b00917.

12. D. Ma and S. Keten, "Stable Micelles Based on a Mixture of Coiled-Coils: The Role of Different Oligomeric States," *Nanoscale* 10, no. 16 (2018): 7589–7596, https://doi.org/10.1039/C7NR09695J.

13. K. A. Scheib, N. A. Tavenor, M. J. Lawless, S. Saxena, and W. S. Horne, "Understanding and Controlling the Metal-Directed Assembly of Terpyridine-Functionalized Coiled-Coil Peptides," *Chemical*

Communications 55, no. 54 (2019): 7752–7755, https://doi.org/10.1039/C9CC03496J.

14. M. Nambiar, M. Nepal, and J. Chmielewski, "Self-Assembling Coiled-Coil Peptide Nanotubes With Biomolecular Cargo Encapsulation," *ACS Biomaterials Science & Engineering* 5, no. 10 (2019): 5082–5087, https://doi.org/10.1021/acsbiomaterials.9b01304.

15. P. Harbury, T. Zhang, P. Kim, and T. Alber, "A Switch Between Two-, Three-, and Four-Stranded Coiled Coils in GCN4 Leucine Zipper Mutants," *Science* 262, no. 5138 (1993): 1401–1407, https://doi.org/10.1126/science.8248779.

16. M. K. Yadav, L. J. Leman, D. J. Price, C. L. Brooks, D. Stout, and M. R. Ghadiri, "Coiled Coils at the Edge of Configurational Heterogeneity. Structural Analyses of Parallel and Antiparallel Homotetrameric Coiled Coils Reveal Configurational Sensitivity to a Single Solvent-Exposed Amino Acid Substitution," *Biochemistry* 45, no. 14 (2006): 4463–4473, https://doi.org/10.1021/bi060092q.

17. J. Liu, Q. Zheng, Y. Deng, C. Cheng, N. R. Kallenbach, and M. Lu, "A Seven-Helix Coiled Coil," *Proceedings. National Academy of Sciences. United States of America* 103, no. 42 (2006): 15457–15462, https://doi.org/10.1073/pnas.0604871103.

18. Y. Zimenkov, S. N. Dublin, R. Ni, et al., "Rational Design of a Reversible pH-Responsive Switch for Peptide Self-Assembly," *Journal of the American Chemical Society* 128, no. 21 (2006): 6770–6771, https://doi.org/10.1021/ja0605974.

19. S. N. Dublin and V. P. Conticello, "Design of a Selective Metal ion Switch for Self-Assembly of Peptide-Based Fibrils," *Journal of the American Chemical Society* 130, no. 1 (2008): 49–51, https://doi.org/10.1021/ja0775016.

20. J. K. Staples, K. M. Oshaben, and W. S. Horne, "A Modular Synthetic Platform for the Construction of Protein-Based Supramolecular Polymers via Coiled-Coil Self-Assembly," *Chemical Science* 3, no. 12 (2012): 3387, https://doi.org/10.1039/c2sc20729j.

21. C. Xu, R. Liu, A. K. Mehta, et al., "Rational Design of Helical Nanotubes From Self-Assembly of Coiled-Coil Lock Washers," *Journal of the American Chemical Society* 135, no. 41 (2013): 15565–15578, https://doi.org/10.1021/ja4074529.

22. M. Nepal, M. J. Sheedlo, C. Das, and J. Chmielewski, "Accessing Three-Dimensional Crystals With Incorporated Guests Through Metal-Directed Coiled-Coil Peptide Assembly," *Journal of the American Chemical Society* 138, no. 34 (2016): 11051–11057, https://doi.org/10.1021/jacs.6b06708.

23. M. Nambiar, L.-S. Wang, V. Rotello, and J. Chmielewski, "Reversible Hierarchical Assembly of Trimeric Coiled-Coil Peptides Into Banded Nano- and Microstructures," *Journal of the American Chemical Society* 140, no. 40 (2018): 13028–13033, https://doi.org/10.1021/jacs.8b08163.

24. M. D. Jorgensen and J. Chmielewski, "Reversible Crosslinked Assembly of a Trimeric Coiled-Coil Peptide Into a Three-Dimensional Matrix for Cell Encapsulation and Release," *Journal of Peptide Science* 28 (2021): e3302, https://doi.org/10.1002/psc.3302.

25. R. W. Curtis, K. L. Scrudders, J. R. W. Ulcickas, G. J. Simpson, S. T. Low-Nam, and J. Chmielewski, "Supramolecular Assembly of his-Tagged Fluorescent Protein Guests Within Coiled-Coil Peptide Crystal Hosts: Three-Dimensional Ordering and Protein Thermal Stability," *ACS Biomaterials Science & Engineering* 8, no. 5 (2022): 1860–1866, https://doi.org/10.1021/acsbiomaterials.2c00155.

26. M. D. Jorgensen and J. Chmielewski, "Co-Assembled Coiled-Coil Peptide Nanotubes With Enhanced Stability and Metal-Dependent Cargo Loading," *ACS Omega* 7, no. 24 (2022): 20945–20951, https://doi.org/10.1021/acsomega.2c01669.

27. J. M. A. Carnall, C. A. Waudby, A. M. Belenguer, M. C. A. Stuart, J. J.-P. Peyralans, and S. Otto, "Mechanosensitive Self-Replication Driven by Self-Organization," *Science* 327, no. 5972 (2010): 1502–1506, https://doi.org/10.1126/science.1182767.

28. W. Helen, P. de Leonardis, R. V. Ulijn, J. Gough, and N. Tirelli, "Mechanosensitive Peptidegelation: Mode of Agitation Controls Mechanical Properties and Nano-Scale Morphology," *Soft Matter* 7, no. 5 (2011): 1732–1740, https://doi.org/10.1039/C0SM00649A.

29. J. Wang, K. Liu, R. Xing, and X. Yan, "Peptide Self-Assembly: Thermodynamics and Kinetics," *Chemical Society Reviews* 45, no. 20 (2016): 5589–5604, https://doi.org/10.1039/C6CS00176A.

30. P. G. Vekilov, "Nucleation," *Crystal Growth & Design* 10, no. 12 (2010): 5007–5019, https://doi.org/10.1021/cg1011633.

31. N. L. Fletcher, C. V. Lockett, and A. F. Dexter, "A pH-Responsive Coiled-Coil Peptide Hydrogel," *Soft Matter* 7, no. 21 (2011): 10210, https://doi.org/10.1039/c1sm06261a.

32. F. Thomas, N. C. Burgess, A. R. Thomson, and D. N. Woolfson, "Controlling the Assembly of Coiled-Coil Peptide Nanotubes," *Angewandte Chemie, International Edition* 55, no. 3 (2016): 987–991, https://doi.org/10.1002/anie.201509304.

33. Y. Tian, F. B. Polzer, H. V. Zhang, K. L. Kiick, J. G. Saven, and D. J. Pochan, "Nanotubes, Plates, and Needles: Pathway-Dependent Self-Assembly of Computationally Designed Peptides," *Biomacromolecules* 19, no. 11 (2018): 4286–4298, https://doi.org/10.1021/acs.biomac.8b01163.

34. V. Castelletto, J. Seitsonen, J. Ruokolainen, and I. W. Hamley, "Alpha Helical Surfactant-Like Peptides Self-Assemble Into PH-Dependent Nanostructures," *Soft Matter* 17, no. 11 (2021): 3096–3104, https://doi.org/10.1039/D0SM02095H.

35. M. Meleties, P. Katyal, B. Lin, D. Britton, and J. K. Montclare, "Self-Assembly of Stimuli-Responsive Coiled-Coil Fibrous Hydrogels," *Soft Matter* 17, no. 26 (2021): 6470–6476, https://doi.org/10.1039/D1SM00780G.